FINAL REPORT

for

Use of Microgravity to Improve the Efficiency and Power Output of Nd-Doped Laser Glasses

CONTRACT: NAG8-779

1 July 1989 to 30 June 1991

Prepared for:

George C. Marshall Space Flight Center
National Aeronautics and Space Administration
Huntsville, AL 35812

Prepared by:

Chandra S. Ray, Principal Investigator
Department of Ceramic Engineering and
Graduate Center for Materials Research
University of Missouri-Rolla
Rolla, MO 65401

20 March 1992

TABLE OF CONTENTS

I. SUMMARY

This report describes the work for the project "Use of Microgravity to Improve the Efficiency and Power Output of Nd-Doped Laser Glasses", Contract NAG8-779, for the period 1 July 1989 to 30 June 1991. The objectives of this research were to:

1) obtain further evidence and understand the science for the reported improvement in chemical homogeneity in glasses prepared in microgravity; and

2) study the feasibility of improving the optical and fluorescence properties, particularly, the limit for Nd^{3+} concentration quenching and threshold energy for laser action for the laser glasses prepared in microgravity.

The anticipated results from this study would provide quantitative data showing the extent to which the power efficiency is increased and the threshold energy is decreased for laser glasses prepared in microgravity. The practical advantage would be to produce laser glasses that would yield higher output power per unit volume than the glasses prepared on earth.

During the two year period of this research, attention was directed to ground-based investigation whose primary purpose was to determine the suitability and conditions for processing these laser glasses in space. This ground-based research was also aimed at developing techniques that would be suitable for handling and analyzing post-flight samples. This report describes that the scientific and technical informations required for planning flight experiments for these glasses have been obtained, and the preparations for handling and analyzing post-flight samples have also been taken. Laser glass compositions in the silicate and phosphate systems, whose processing parameters are well within the capability of the flight instruments presently available, have been developed. Instruments required for measuring the fluorescence properties of interest have been constructed. The optical and fluorescence

properties for the glasses which have been planned to process in space, have been measured and made available for comparative property analysis. Techniques to obtain reliable fluorescence data even for small samples (<6 mm diameter) have been developed, should the samples obtained from flight experiments are restricted to small size. To accomplish the final objective of this work, i.e., to study the feasibility of improving the fluorescence efficiency and output power for laser glasses prepared in microgravity, a Flight Investigator Proposal has been submitted to the National Aeronautics and Space Administration (NASA) in response to the announcement NRA-91-OSSA-20 of 30 August 1991. If this request is granted, laser glasses containing different concentration of Nd_2O_3 will be prepared in space. The optical and fluorescence properties for the flight samples will be measured using the instruments and techniques developed in this ground-based research. A comparison of these properties for the flight samples with those determined in this investigation for the identical glasses prepared on earth will indicate the extent to which the fluorescence properties for the glasses prepared in space could be improved.

II. INTRODUCTION

Glass is an efficient host material for solid state lasers.[1-3] The active element in a laser glass is a solid solution of fluorescent ions in a glass host matrix. The effect of various ions such as Nd^{3+}, Gd^{3+}, Ho^{3+}, Er^{3+}, Yb^{3+}, etc. in glasses has been studied,[4-8] but Nd^{3+} has proven to be most effective. The most important emission line for Nd^{3+} is at 1060 nm (in the infrared) involving the transition $^4F_{3/2} \rightarrow {}^4I_{11/2}$.

It is well known that the simplest way to improve the power efficiency of a laser glass is to increase the concentration of the fluorescence ions (Nd^{3+} in this case) in the glass. However, this effort is always nullified by the increasing fluorescence self-quenching with increasing Nd^{3+} concentration.[3,9,10] The concentration quenching sets an upper limit to the Nd^{3+} concentration above which the power efficiency of the laser glass decreases with further increase in the Nd^{3+} concentration.

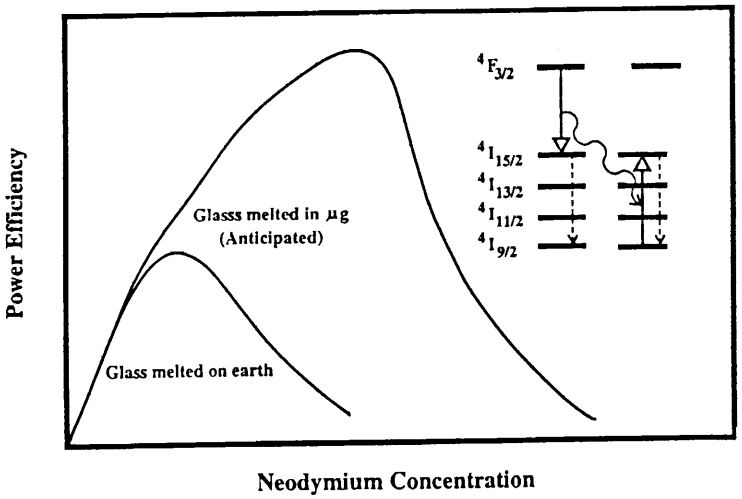

Fig. 1. A schematic diagram of concentration quenching for a Nd-doped laser glass upper right corner. The glass melted in microgravity is expected to have higher concentration quenching limit.

The mechanism for concentration quenching of Nd^{3+} has been well known as a resonance interaction between the $^4F_{3/2} \rightarrow {}^4I_{15/2}$ transition of an excited Nd^{3+} ion and the $^4I_{9/2} \rightarrow {}^4I_{15/2}$ transition of a nearby unexcited Nd^{3+} ion. This resonance interaction serves to deplete the $^4F_{3/2}$ levels,[1-3,9-12] and both ions decay nonradiatively back to the ground state ($^4I_{9/2}$). The quenching process is shown schematically in the upper right

corner of Fig. 1. An increase in this nonradiative transition associated with concentration quenching decreases the fluorescence efficiency and fluorescence lifetime, and consequently, increases the threshold energy for laser action.

This interaction or quenching increases with decreasing separation between the ions. It has been suggested that this interaction occur when the separation between two neighboring Nd^{3+} ions is lower than a certain critical value, typically 8.5 to 9.5 Å.[3] Our calculations show that at least 14 to 15 wt% Nd_2O_3 is required to reach the critical Nd^{3+} separation of $\approx$9 Å in a typical silicate and phosphate laser glass if the Nd^{3+} ions are homogeneously distributed. But for the laser glasses prepared on earth, concentration quenching occurs when Nd_2O_3 content is far below this critical concentration. This is believed[13] due to the formation of the Nd^{3+} clusters (chemically heterogeneous regions) in the laser glasses prepared on earth. With increasing Nd_2O_3 content, the number of such clusters in the glasses increases, causing a continuous reduction in the fluorescence output.

Fluorescence quenching is also caused by certain impurities in the glass, such as platinum. This is known as impurity quenching. The impurities in the glass either scatter or absorb a part of the fluorescence output and then relax through a nonradiative transition. These impurities also interact with the input energy in the same way and prevent much of the energy from being used for pumping the fluorescence ions. This also effectively increases the threshold for laser action. The energy absorbed by the impurities and its subsequent transfer to the lattice by nonradiative transition could even damage the laser host material by localized overheating. The contamination of a glass melt by the impurities introduced from the platinum or ceramic crucible is one of the major factors for the failure or damage of a laser glass during operation.

Glasses melted in microgravity have been reported[13-17] to be more chemically homogeneous compared to those prepared at one-g (on earth). This means that the Nd^{3+} ions

will be more homogeneously distributed in a laser glass prepared in micro-g and it should be possible to incorporate more Nd^{3+} ions in the glass before ion-ion interactions become significant, i.e., before significant fluorescence quenching occurs. The uniform distribution of Nd^{3+} ions in the glass is expected to increase the limit for concentration quenching and, hence, to produce glasses with increased output power per unit volume. In fact, it has been demonstrated[13] that more than 2 to 3 wt% Nd_2O_3 added to a phosphate laser glass prepared on earth reduces significantly the lifetime of Nd^{3+} fluorescence (a direct consequence of concentration quenching), while no detectable change in lifetime was observed when up to 10 to 12 wt% Nd_2O_3 was added to the same glass melted in micro-g.

In addition, microgravity provides the opportunity of preparing glasses containing an extremely low level of impurities. Impurities introduced from the container into the melt are reported[16] to be confined only in the close vicinity of the melt-container interface. Absence of gravity-driven convection in micro-g reduces the rate of material transport and the bulk of the melt (glass) remains essentially free from impurities. This, in turn, should result in a suppression or elimination of the impurity quenching (of fluorescence) and impurity-induced damage of the laser glasses.

Based on the above ideas, an investigation which was funded by NASA (Contract NAG8-779) from 1 July 1989 to 30 June 1991 (two years) was undertaken. The primary objectives of that research were to:

1) obtain further evidence and understand the science for the reported improvements in chemical homogeneity in glasses prepared in microgravity;
2) increase the limit of Nd^{3+} ions concentration quenching in various glasses (silicate, phosphate, and borate) processed in microgravity compared to that observed for

identical glasses prepared on earth, and, hence, to prepare laser glasses with increased output power per unit volume and reduced threshold energy; and

3) decrease the threshold energy for laser action and further increase the output power by suppressing or eliminating impurity quenching in glasses processed in micro-g.

The anticipated results from this study would provide quantitative data showing the extent to which the power efficiency is increased and the threshold energy is decreased for laser glasses prepared in microgravity. The practical advantage would be to produce laser glasses that would yield higher output power per unit volume than the glasses melted on earth.

During the period of this research, emphasis was given to ground-based investigation whose primary purpose was to determine the suitability and conditions for processing laser glasses in space and develop techniques suitable for handling and analyzing post-flight samples. Attention in the present research, therefore, was directed to:

1) Develop laser glass compositions which would be suitable for use in flight experiments,

2) Design and construct instrumentations for measuring fluorescence efficiency and lifetime of Nd^{3+} fluorescence,

3) Measure optical and fluorescence properties such as the refractive index, absorption, fluorescence lifetime, fluorescence intensity, and the limit for concentration quenching for the glasses developed in 1) above and prepared conventionally (i.e., melting in a platinum crucible and casting onto a steel plate) on earth, so as to make these data available for comparison with those for the glasses prepared in microgravity.

The results obtained and the achievements accomplished in this research are described in the following section.

III. EXPERIMENT AND RESULTS

It is mentioned before that during the period of this research, the primary emphasis was given to ground-based investigation such as composition selection, glass preparation, construction of experimental apparatus, and determination of fluorescence concentration quenching. The experiments conducted and the results obtained for this research are summarized and discussed below.

A. Preparation of Silicate and Phosphate Laser Glasses

Two compositions were developed from the silicate and phosphate systems, namely, "LG" ($60.14SiO_2$-$2.53Al_2O_3$-$27.32Li_2O$-$9.86CaO$-$0.15CeO_2$) and "LP" ($50.0P_2O_5$-$3.0Al_2O_3$-$27.0Li_2O$-$20.0CaO$), mol%, respectively, as the host glass compositions for this investigation. Different amounts of Nd_2O_3 (0.25 to 4.0 mol%) were added to these glasses. The selection of the host glass compositions was based on two considerations: 1) the suitability for laser application, such as stability against moisture, high resistance against thermal shock, and extremely low absorption (especially at the absorption and emission wavelength of Nd^{3+} ions), etc., and 2) the melting temperatures which should be well within the capability of the furnace presently used for flight experiments. The silicate base glass was selected to have the similar composition as that of the Owens-Illinois ED-2 laser glass so that the experimental results can be directly compared with those reported in the literature.[18,21,23] In the phosphate glass, the Li_2O, CaO, and Al_2O_3 contents were maintained comparable to those of the silicate glass.

The glasses were prepared by melting well-mixed batches in a platinum crucible at 1400°C for 4 hrs for the silicate glasses and 1250°C for 2 hrs for the phosphate glasses. The melts were bubbled with oxygen for at least 1 hr to ensure homogeneity. After melting, the melt was cast onto a steel plate to form glass and then annealed at 450°C for 2 hrs to eliminate

residual stresses. The glasses obtained were transparent, free from bubbles and crystal inclusions, and chemically durable. The dissolution rate for the phosphate glasses measured in distilled water at 50°C was $\sim 10^{-7}$ gm-cm^{-2}-min^{-1}, which is comparable to that of the commercial soda-lime-silica glass. The dissolution rate for the silicate laser glasses was not measured since the chemical durability of the silicate glasses is, in general, better than that of the comparable phosphate glasses.

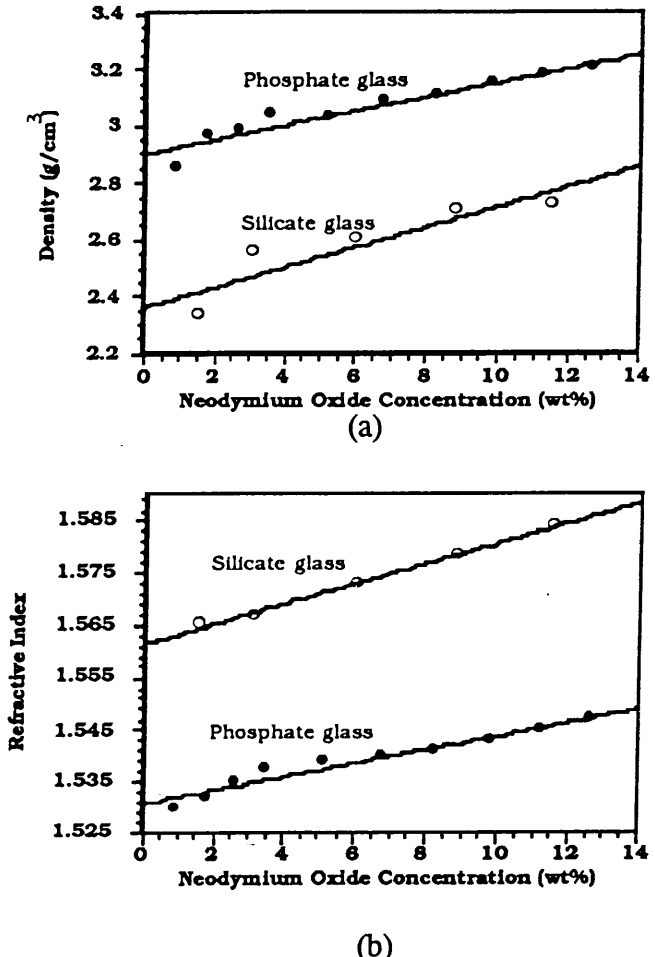

Fig. 2. The density and refractive index of the LG and LP glasses as a function of Nd_2O_3 concentration.

The refractive index and density of these glasses were also measured using Becke-line technique and Archimedes method, respectively, and are shown in Fig. 2a and b as a function of Nd_2O_3 content. As expected, both the density and refractive index for the silicate and phosphate laser glasses increased with increasing Nd_2O_3 concentration.

B. Measurements of Absorption Spectra

The optical absorption measurements for the glasses were made in the wavelength range between 400 and 950 nm using a Beckman Model-26 spectrophotometer. The spectrophotometer was calibrated at 370 nm using standard K_2CrO_4 solution in 0.05 N KOH. Polished glass samples of size $\sim$20 x 10 x 2 mm^3 were used for these measurements.

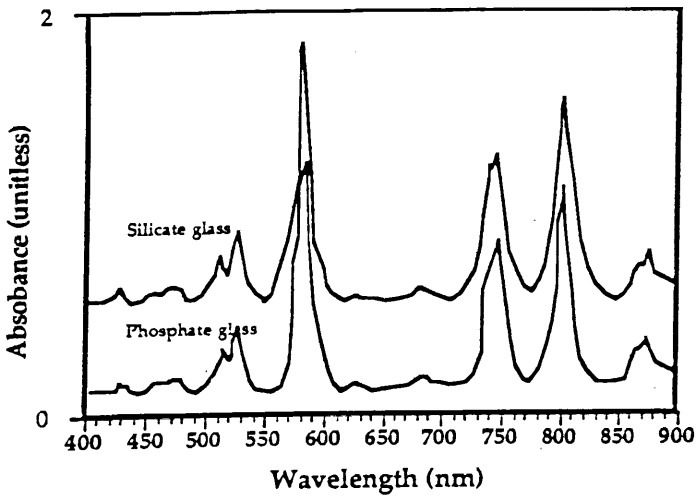

Fig. 3. The typical absorption spectra of Nd^{3+} in the LG and LP glasses.

The typical absorption spectra for LG and LP glasses containing 2 mol% Nd_2O_3 are shown in Fig. 3. It is evident from Fig. 3 that the Nd^{3+} absorption spectra for the silicate and phosphate glasses are, in general, very similar. Also, no significant changes in the absorption spectra with changing Nd^{3+} concentration were observed for any of the silicate and phosphate glasses. However, minor differences in the absorption coefficient and bandwidth between the spectra for the silicate and phosphate glasses were noted.

C. Measurements of Fluorescence Spectra and Fluorescence Lifetime, τ_f

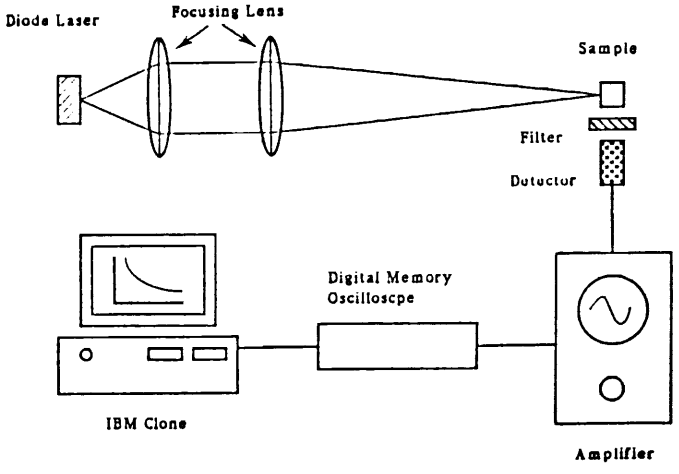

Fig. 4. Schematic of experimental setup for fluorescence lifetime measurement.

The fluorescence lifetime, τ_f, and the relative fluorescence intensity, I_f, for these glasses were measured using polished glass samples of size ~ 10 x 5 x 2 mm and an experimental setup designed and constructed by ourselves. The complete arrangement of the experimental setup is shown in Fig. 4 in block diagrams.

The glass samples were irradiated by a radiation of nominal wavelength 805 nm emitted by a diode laser* and the resulting fluorescence was filtered and detected using a silicon photodetector at the direction perpendicular to the incident radiation to avoid contamination of the residual 805 nm radiation from the diode laser. The signal from the detector was amplified and then sent to a digital memory oscilloscope (DMO) which was interfaced with an IBM clone computer. The fluorescence spectra and the intensity decay curves were then recorded and stored in the IBM clone computer.

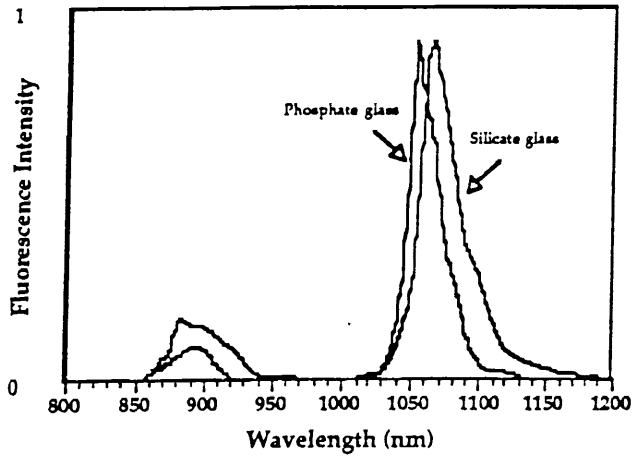

Fig. 5. Typical $^4F_{3/2} \rightarrow {}^4I_{11/2}$ (1020-1150 nm) and $^4F_{3/2} \rightarrow {}^4I_{9/2}$ (850-950 nm) transition fluorescence spectra.

The fluorescence spectra were measured at wavelengths between 800 and 1200 nm and are shown in Fig. 5 for the silicate and phosphate glasses containing 0.5 mol% Nd_2O_3. The Nd^{3+} fluorescence for the $^4F_{3/2} \rightarrow {}^4I_{11/2}$ and $^4I_{9/2}$ transitions appeared at 1052 and 891 nm, respectively, for the LP glass and at 1062 and 880 nm, respectively, for the LG glass. No significant change in the peak positions with changing Nd_2O_3 concentration was observed for either of the LP and LG glasses. The effective fluorescence linewidth, $\Delta\lambda_{eff}$, was calculated using numerical integration of the fluorescence line shapes and is shown in Fig. 6 and Table I for both the LP and LG glasses as a function of Nd_2O_3 concentration. It is observed that the phosphate glasses have narrower linewidth ($\sim$265 cm^{-1}) compared to the silicate glasses ($\sim$340 cm^{-1}), but the linewidths of the fluorescence peaks for each glass family are nearly independent of Nd_2O_3 concentration.

---

*Spectra Diode Labs, SDL-2410-C.

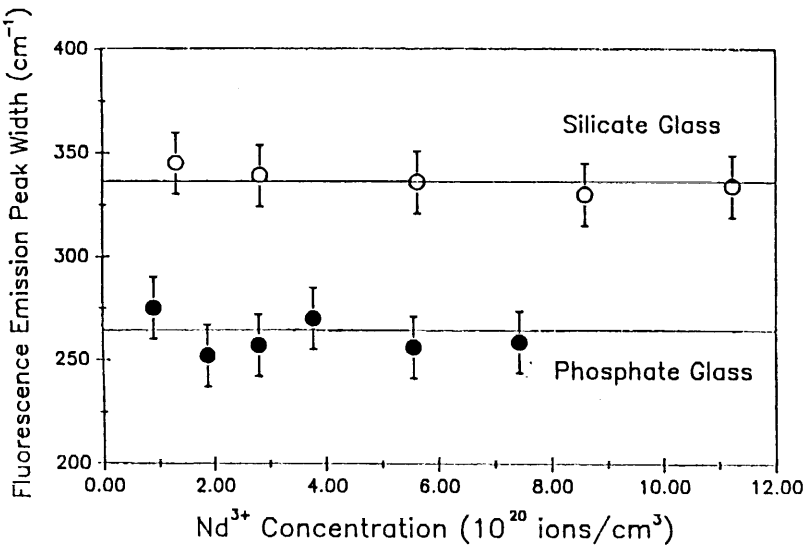

Fig. 6. Effective fluorescence linewidth of $^4F_{3/2} \rightarrow {}^4I_{11/2}$ transition for the Nd-doped LG and LP glasses.

The lifetime, τ_f, of fluorescence at 1060 nm (which is the primary laser radiation emitted by a Nd-doped laser glass) was measured by recording the relative intensity, I, of the emitted fluorescence at 1060 nm for up to 2000 μs after the glass sample was irradiated. The fluorescence lifetime, τ_f, is related to I through a simple exponential decay relation as:

$$I = I_o \exp(-t/\tau_f) + C \qquad (1)$$

where the pre-exponential factor, I_o (instantaneous absolute intensity) and the constant, C, have less practical significance for the measurements of τ_f. A typical exponential decay curve for the LG glass (silicate) containing 0.5 mol% Nd_2O_3 is shown in Fig. 7a. The time after which the intensity decreases to (1/e) of its original value is the lifetime of fluorescence, τ_f. A logarithmic form of Eq. (1) should be a straight line, from the slope of which τ_f can also be determined. The logarithmic form of the measured decay curve in Fig. 7a is produced in Fig. 7b which shows an excellent linearity in the entire range of time for measurements ($\sim$2000 μs). The value of τ_f determined using either Fig. 7a or 7b is in excellent agreement and is 299.3 $\pm$ 0.5 μs for the LG glass doped with 0.5 mol% Nd_2O_3.

It was observed that the intensity data for the silicate glasses did not follow a simple exponential decay relation as shown in Eq. (1) for the glasses containing higher Nd_2O_3. This

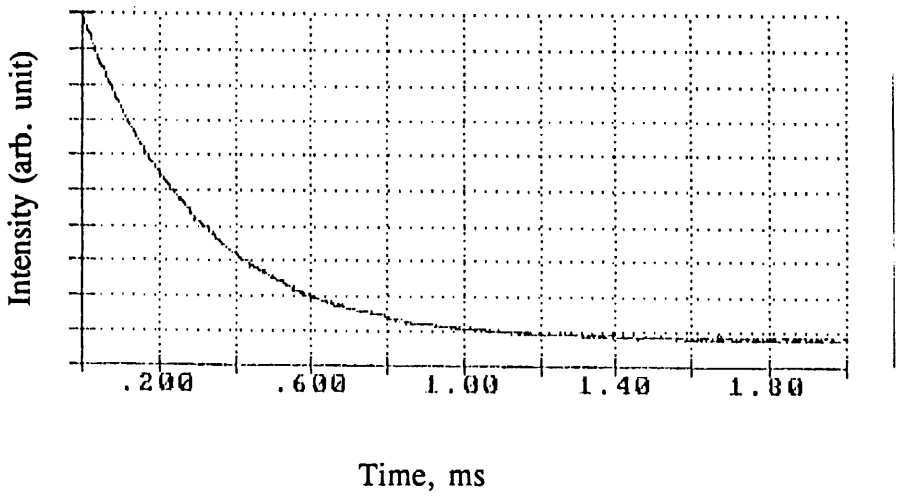

Fig. 7a. Intensity decay curve of the 1060 nm Nd^{3+} fluorescence for the LG glass containing 0.5 mol% Nd_2O_3.

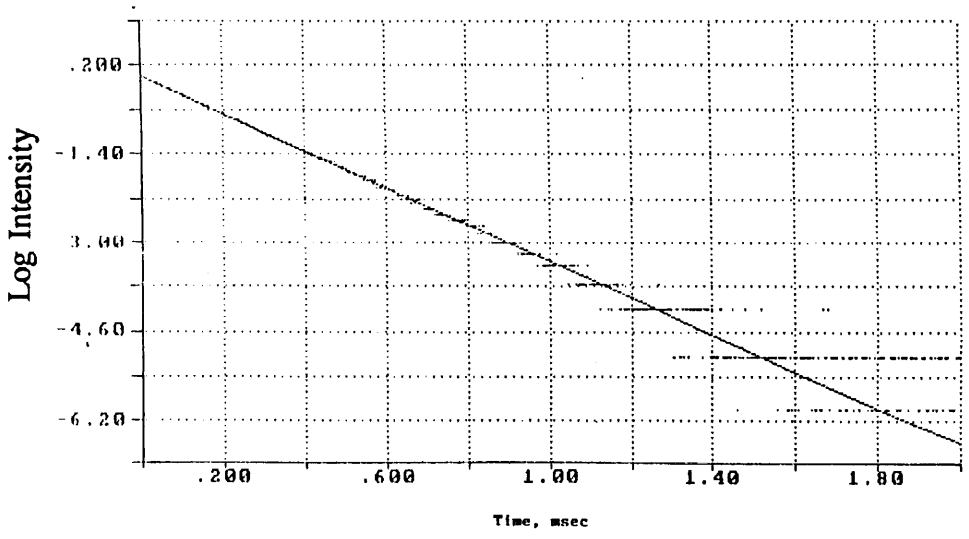

Fig. 7b. Logarithmic plot of Fig. 7a.

is, however, in agreement with Nd^{3+} fluorescence decay observed in a variety of hosts.[21,23,24] Employing a least squares computer program, we found that these silicate glasses followed a double exponential decay relation of the form:

$$I = I_1 \exp [- t/(\tau_f)_1] + I_2 \exp [- t/(\tau_f)_2] \quad (2)$$

Values of $(\tau_f)_1$ and $(\tau_f)_2$ determined for the glasses containing different concentration of Nd_2O_3 are shown in Table I. For the silicate glasses containing $Nd_2O_3 \leq 0.5$ mol%, the single exponential decay relation (Eq. (1)) correctly describes the experimental data points. The use of the double exponential decay relation (Eq. (2)) for these glasses yields $(\tau_f)_1$ and $(\tau_f)_2$ nearly identical, which are in agreement with the value determined using the single exponential decay relation. For the glasses containing $Nd_2O_3 > 0.5$ mol%, the double exponential decay relation (Eq. (2)) represents a better fit and yield widely different values for $(\tau_f)_1$ and $(\tau_f)_2$. There is no theoretical justifications which one of $(\tau_f)_1$ and $(\tau_f)_2$ represents the "real" fluorescence lifetime, but the "first e-fold decay time" (the short decay time component) is usually used to represent the fluorescence lifetime in these cases.[23,24]

In contrast to silicate glasses, almost all the experimental decay curves for phosphate glasses containing different concentration of Nd_2O_3 can be fitted to a single exponential decay law and the use of double exponential relation yields $(\tau_f)_1$ and $(\tau_f)_2$ nearly identical, see Table I. The dependence of the 1060 nm fluorescence lifetime, τ_f, on the Nd_2O_3 concentration is shown in Fig. 8a for both the silicate and phosphate glasses. For silicate glasses containing $Nd_2O_3 > 0.5$ mol%, the short decay time component, $(\tau_f)_1$, was used as τ_f in Fig. 8a. It is observed that τ_f decreases continuously with increasing Nd_2O_3, which is a consequence for the effect of concentration quenching. Although the limit for concentration quenching could not be precisely determined from these measurements because of a smooth decrease of τ_f with

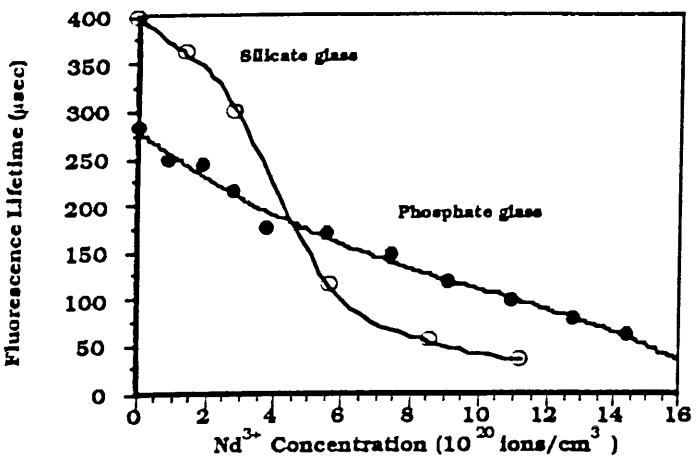

(a)

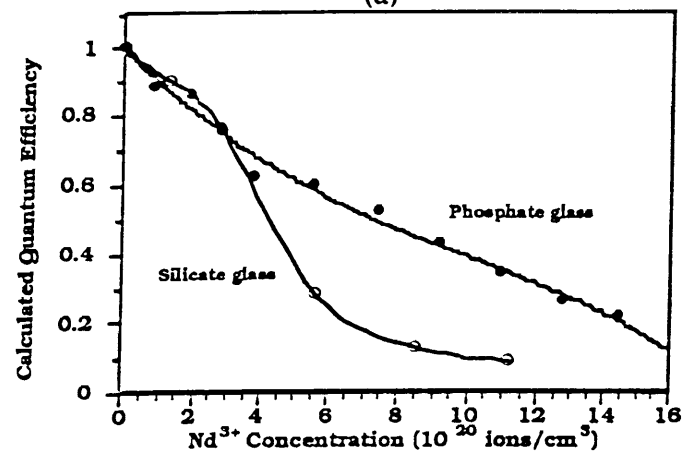

(b)

Fig. 8. Dependence of the fluorescence lifetime and calculated quantum efficiency for the Nd $^4F_{3/2} \rightarrow {}^4I_{11/2}$ transition in the LG and LP glasses.

increasing Nd_2O_3, the effect of concentration quenching appeared to be more prominent and to occur at a lower concentration of Nd_2O_3 for the silicate glasses compared to those for the phosphate glasses.

The limit for concentration quenching is usually determined by plotting the relative fluorescence intensity as a function of Nd_2O_3 concentration.[12] The plots of the measured relative intensity, I_f, of the emitted 1060 nm fluorescence for the silicate and phosphate glasses are shown in Fig. 9a as a function of Nd^{3+} concentration. Figure 9a shows that I_f initially increases with increasing Nd^{3+} concentration and then decreases when the Nd^{3+} concentration exceeds a critical value which may be considered as the limit for concentration quenching. As determined from Fig. 9a, concentration quenching for these silicate and phosphate glasses occurs at Nd^{3+} concentration $\sim 2.85 \times 10^{20}$ and 9.00×10^{20} cm^{-3}, respectively, which correspond to Nd_2O_3 content ~ 0.49 and 2.30, mol%, respectively. The higher concentration limit for fluorescence self quenching in the phosphate glass indicates that the Nd^{3+} fluorescence concentration quenching is less pronounced in the phosphate glass compared to that for the

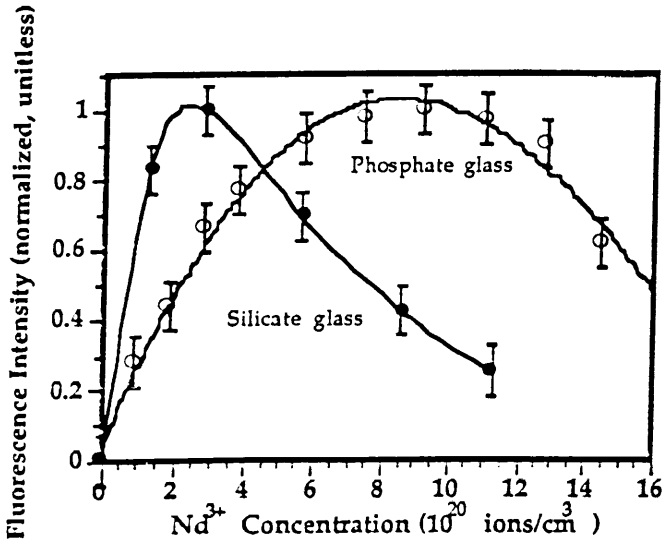

Fig. 9a. Relative fluorescence intensity for the Nd $^4F_{3/2} \rightarrow {}^4I_{11/2}$ transition as a function of Nd^{3+} concentration in the LG and LP glasses.

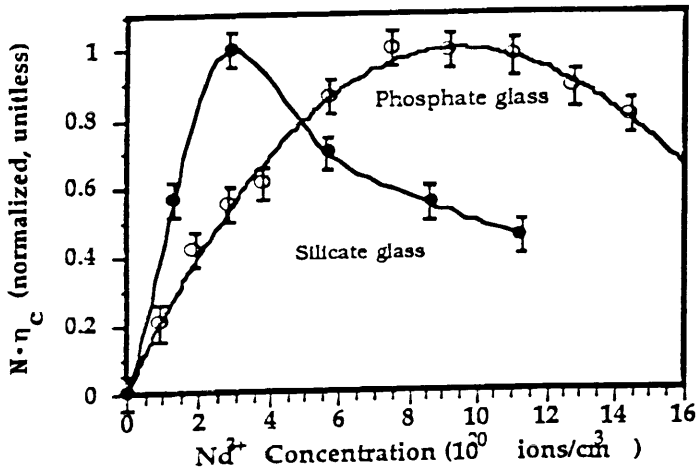

Fig. 9b. Plot of $N \cdot \eta_c$ as a function of N (Nd^{3+} concentration) for the $^4F_{3/2} \rightarrow {}^4I_{11/2}$ transition in the LG and LP glasses.

silicate glass, which has also been observed qualitatively from the fluorescence lifetime measurements, see Fig. 8a.

D. Calculation of Radiative Properties of Nd^{3+} from Absorption Measurements

In order to obtain further information about the transitions from the $^4F_{3/2}$ to different terminal levels of the neodymium ion embedded in the glass matrix, the probability, branching ratio, and radiative lifetime for these transitions were calculated using the Judd-Ofelt (J-O) model.[18,19,23] The J-O model is a semi-empirical method in which experimentally determined absorption coefficients are utilized to calculate the radiative properties. Several investigators[18,19,23] have discussed the usefulness of J-O procedure for such calculations and found that the calculated values are in good agreement with the measured properties within an accuracy of $\pm 10\%$.

A brief summary of the pertinent equations to be used for these calculations is presented here using the notations used in ref. 18. The radial integral and energy denominators which

appear in the perturbation theory as well as in the crystal field splitting terms are characterized by three empirical coefficients, Ω_2, Ω_4, and Ω_6 known as intensity parameters. These parameters can be determined by a least-squares fit of the following relation:

$$\int_{\text{band}} k(\lambda)d\lambda = \frac{8N\pi^3e^2\bar{\lambda}}{3ch(2J+1)n}\left[\frac{(n^2+2)^2}{9}\right]\sum_{t=2,4,6}\Omega_t|\langle(S,L)J||U^{(t)}||(S',L')J'\rangle|^2 \quad (3)$$

where, $k(\lambda)$ is the wavelength dependent absorption coefficient, N is the Nd^{3+} concentration in cm^{-3}, $\bar{\lambda}$ is the mean wavelength of the absorption band, J is the total angular momentum quantum number of the lower level, n is the index of refraction at the wavelength $\bar{\lambda}$, h is the Planck's constant, c is the speed of light, e is the electronic charge, and $\langle(S,L)J||U^{(t)}||(S',L')J'\rangle$ are the matrix elements of the doubly reduced unit tensor operator, the values of which for the needed Nd^{3+} levels are available in the literature.[25] Once the parameters Ω_2, Ω_4, and Ω_6 are determined, the following radiative properties of Nd^{3+} in the glasses can be evaluated.

1. Spontaneous Emission Probability from an initial level $|(S',L')J'\rangle$ to a final level $|(S,L)J\rangle$:

$$A[(S',L')J';(S,L)J] = \frac{64\pi^4e^2n}{3h(2J'+1)\bar{\lambda}^3}\left[\frac{(n^2+2)^2}{9}\right]\sum_{t=2,4,6}\Omega_t|\langle(S',L')J'||U^{(t)}||(S,L)J\rangle|^2 \quad (4)$$

2. Fluorescence Branching Ratio, β, for transition from an initial level $|(S',L')J'\rangle$ to a lower final level $|(S,L)J\rangle$:

$$\beta[(S',L')J'] = \frac{A[(S',L')J';(S,L)J]}{\sum_{S,L,J} A[(S',L')J';(S,L)J]} \quad (5)$$

This parameter measures the fractional probability of a particular transition compared to the total probability for all the radiative transitions involved.

3. Radiative Lifetime, τ_r:

$$\tau_r = \left\{ \sum_{S,L,J} A\,[(S',L')J';(S,L)J] \right\}^{-1} \tag{6}$$

τ_r is a measure of the average time an electron spends in a metastable level that gives rise to a radiative transition and is reciprocal of the total probability for radiative transitions.

4. Radiative Quantum Efficiency, η_c, of the $|(S',L')J'>$ level:

$$\eta_c = \tau_f/\tau_r \tag{7}$$

where τ_f is the measured fluorescence lifetime which includes all the radiative, nonradiative, and ion-ion interaction relaxation processes.

5. Peak-Induced Emission Cross Section, σ_p, for the Nd^{3+}, $^4F_{3/2} \rightarrow {}^4I_{11/2}$ transition:

$$\sigma_p(\lambda_p) = \frac{\lambda_p^2}{8\pi c n^2 \Delta\lambda_{eff}} A\,[(^4F_{3/2});(^4I_{11/2})] \tag{8}$$

where $\Delta\lambda_{eff}$ is the effective fluorescence linewidth determined by integrating the fluorescence line shape and dividing by the intensity at the peak fluorescence wavelength of emission, λ_p. The induced emission cross section, σ_p, is one of the most important parameters for laser design, since an increasing σ_p increases the spatial growth of intensity for laser radiation.

The area under the absorption curves in Fig. 3 was measured using a planimeter to a precision of about 5%. Using the measured area under the absorption curves, Nd^{3+} concentration and refractive index (Fig. 2b), the intensity parameters Ω_2, Ω_4, and Ω_6 were

calculated using Eq. (3) and are shown in Table II. The Nd^{3+} concentration was determined from the density and Nd_2O_3 content in the glass (Fig. 2a). Using these calculated values for Ω_2, Ω_4, and Ω_6, the radiative properties of Nd^{3+} such as the spontaneous emission probability, A, branching ratio, β, and radiative lifetime, τ_r, for the transitions from $^4F_{3/2}$ to $^4I_{9/2}$, $^4I_{11/2}$, $^4I_{13/2}$, and $^4I_{15/2}$ terminal levels which correspond to fluorescence emissions at about 880, 1060, 1350, and 1800 nm, respectively, were calculated (see Eqs. (4-6)) and the results are shown in Table III as a function of Nd_2O_3 concentration for both the silicate and phosphate glasses. As expected, the emission probability and, hence, the branching ratio for the 1060 nm emission is the highest among all other emissions of the Nd^{3+} ions in these glasses. Table III shows that the radiative properties for these glasses are nearly independent of the concentration of Nd^{3+}, but depend on the host glass composition. Compared to the results for the silicate glasses, the Ω and A values are larger and τ_r smaller for the phosphate glasses, see Tables II and III. It is to be noted that the calculated radiative properties for the silicate glass containing 0.5 mol% Nd_2O_3 (LG-0.5) are in excellent agreement with those reported for the commercial ED-2 glass[18] whose composition is similar to that of the LG-0.5 glass studied in the present investigation.

The radiative lifetime, τ_r, is a parameter which should not change with Nd^{3+} concentration. On the other hand, the measured lifetime, τ_f, results from all type of emissions involved such as those resulting from radiative and multiphonon relaxations, and ion-ion interactions. The multiphonon relaxation rate for the $^4F_{3/2}$ manifold of Nd^{3+} is anticipated to be very small,[18] since the energy gap for the $^4F_{3/2}$ manifold is very high (~ 4700 cm^{-1}) compared to the general cut off energy for optical phonons (~ 1200 cm^{-1}). In other words, the observed decrease in τ_f with increasing Nd^{3+} (Fig. 8a) is primarily caused by ion-ion interaction (concentration quenching). This also means that τ_f should approach to the radiative lifetime τ_r when the relaxation via Nd-Nd interaction will vanish, i.e., $\tau_f \rightarrow \tau_r$ in the limit $N \rightarrow O$. When

the measured fluorescence lifetime, τ_f, is extrapolated back to zero Nd^{3+} concentration (see Fig. 8a), it yields values ~400 and 280 μs for the silicate and phosphate glasses, respectively, which are very close to the average radiative lifetime, τ_r (394 $\pm$ 26 and 287 $\pm$ 7 μs for the silicate and phosphate glasses, respectively), calculated by J-O technique, see also Table III.

The radiative quantum efficiency $\eta_c = \tau_f/\tau_r$ (Eq. (7)) should approach unity as the concentration of Nd^{3+} approaches to zero since in this limit $\tau_f \rightarrow \tau_r$. Like τ_f, η_c should then decrease with increasing Nd^{3+} concentration. Using the measured value of τ_f and the calculated average value of τ_r, η_c for these glasses were determined and is plotted in Fig. 8b as a function of Nd^{3+} concentration. As expected, these plots are quite similar to the plots of τ_f (Fig. 8a) and exhibit clearly the effect of ion-ion interaction (concentration quenching) which appears to be more prominent in the silicate glass compared to that in the phosphate glass.

E. Estimation of the Limit for Concentration Quenching

The spatial growth of intensity of the laser radiation in a medium depends primarily upon the radiative quantum efficiency, η_c, and the gain or amplification coefficient of the medium. A high η_c (which is a ratio of the probabilities for the radiative to all possible relaxations) converts a high fraction of the absorbed light into fluorescence and a high gain coefficient extracts a high fraction of the stored energy from the system and increases the intensity of the fluorescence. The gain coefficient depends upon the population inversion (in fact, upon the inversion density) which, in turn, depends upon the concentration, N, of the Nd^{3+} ions. It is, therefore, reasonable to assume that the product $N \cdot \eta_c$ can be used as a figure of merit to evaluate the effect of Nd^{3+} concentration on the performance of a laser glass. The product $N \cdot \eta_c$ for the LG and LP glasses studied in the present investigation is plotted in Fig. 9b as a function of Nd^{3+} concentration, which is identical to the curve obtained by plotting the relative intensity

of fluorescence, I_f, at 1060 nm as a function of Nd^{3+} concentration, Fig. 9a. The limit for concentration quenching determined using Fig. 9b is also same as that determined using Fig. 9a, namely, 2.85 x 10^{20} and 9.00 x 10^{20} Nd^{3+} ions/cm^3 for the silicate and phosphate glasses, respectively (see also Table IV). These results indicate that the plot of $N \cdot \eta_c$ vs. N can be used to determine the limit for concentration quenching in laser glasses with a reasonable accuracy. The advantage of this method is that it does not require a precise control for the preparation of samples to be investigated as opposed to what is required for the measurements of I_f. This advantage enables one to investigate smaller size samples (<6 mm diameter) such as those presently obtainable from containerless experiments on earth (maximum size obtainable ~3 to 4 mm diameter) or in space (maximum size obtainable ~6 to 8 mm diameter). Although the measurements of I_f can also be performed on samples of small size (~6 mm diameter), the geometries (cross sectional diameter, thickness) of different samples containing different amounts of Nd_2O_3 should be maintained precisely constant so that the fluorescence intensities for the samples can be directly compared. Maintaining constant geometry is a difficult task for samples of small size.

F. Crystallization Measurements

The crystallization behavior of the glasses was studied using differential thermal analysis (DTA) and x-ray diffraction (XRD) as a function of Nd_2O_3 content. Both the silicate and phosphate glasses were surface crystallized during heat treatment, and the phosphate glasses were seriously deformed due to softening before crystallization. This indicates that the phosphate glasses are more resistant to crystallization than the silicate glasses.

The DTA curves obtained at heating rate 10°C/min are shown in Figs. 10 and 11 for the silicate and phosphate glasses, respectively. There are three main crystallization peaks appearing

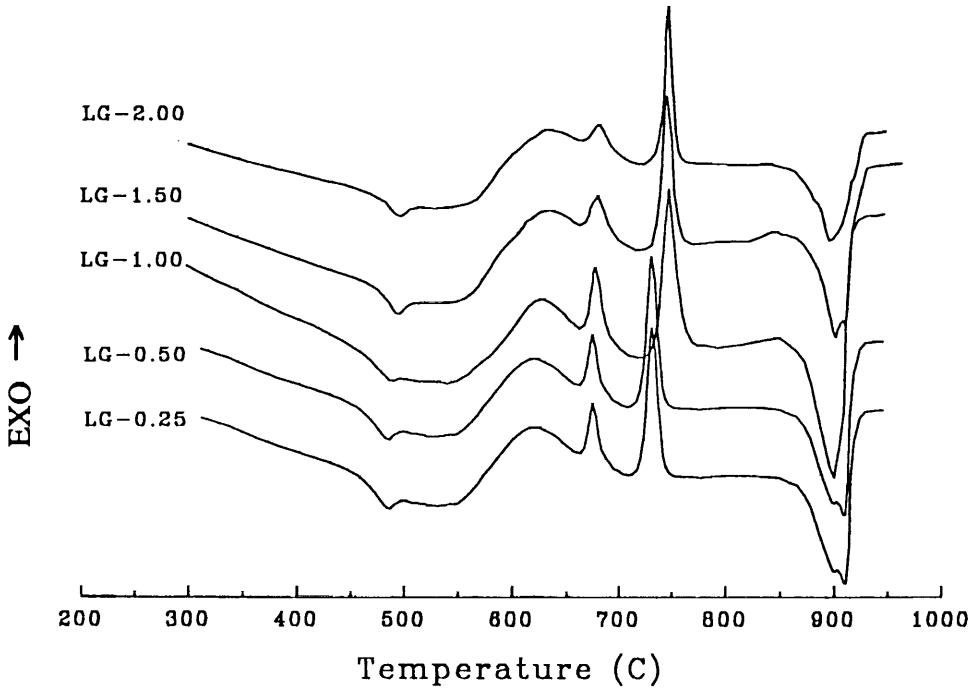

Fig. 10. DTA crystallization of the LG glasses containing different concentration of Nd_2O_3.

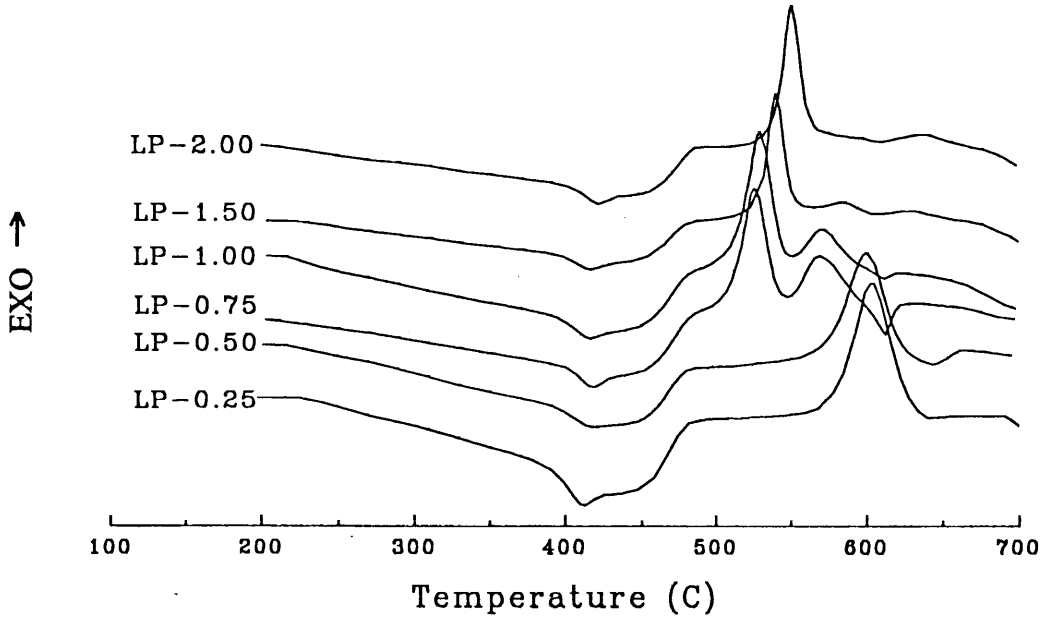

Fig. 11. DTA crystallization curves of the LP glasses containing different concentrations of Nd_2O_3.

for the silicate glasses, a broad crystallization peak between 550 and 700°C with a peak maxima at ~640°C, and two sharp peaks with maxima at ~685 and 750°C. As analyzed by XRD, these peaks are found to correspond to the crystallization of $Li_2O \cdot SiO_2$ (peak maxima at 640°C), $3CaO \cdot Al_2O_3 \cdot 3SiO_2$ (peak maxima at 685°C), and the β-quartz solid solution (peak maxima at 750°C). Figure 10 also shows that the DTA curves for these glasses are nearly identical, i.e., the crystallization behavior for the Nd_2O_3 doped silicate glasses is independent of Nd_2O_3 content. The only minor change observed is a little shift of the glass transition temperature, T_g, towards higher temperature with increasing Nd_2O_3, from 460.5 to 485°C for an increase of Nd_2O_3 from 0.25 to 2.00 mol%. The height of the crystallization peak at 685°C remained constant for Nd_2O_3 content up to 1.00 mol%, which then decreased with further increase of Nd_2O_3.

Unlike silicate glasses, the DTA curves for the phosphate glasses (Fig. 11) show a significant change with Nd_2O_3 concentration. For the glasses containing 0.25 and 0.5 mol% Nd_2O_3, there was only crystallization peak appearing between 560 and 650°C with peak maximum at ~600°C. For glasses containing Nd_2O_3 >0.5 mol%, several peaks were found to appear, one sharp and large exothermic peak with maximum at ~530°C, one weak exothermic peak with maximum at ~570°C, and an endothermic peak with maximum at ~612°C. With further increase of Nd_2O_3, the weak crystallization peak at 570° and the endothermic peak at 612°C were found to decrease and disappear for glasses containing Nd_2O_3 >1.5 mol%. The maximum peak temperature for the large exotherm slowly shifted towards higher temperature with increasing Nd_2O_3 content, from 530 to 556°C for an increase of Nd_2O_3 from 0.75 to 2.00, mol%. Because of the complexity of the x-ray diffraction patterns, the crystalline phases in the devitrified samples for these phosphate glasses could not be identified. Another interesting feature common to all the DTA curves for these glasses is the presence of an exothermic shoulder around 480°C, the reason for which could not be understood at this

time. The glass transition temperature, T_g, for these phosphate glasses was independent of Nd_2O_3 content and was ~420°C.

IV. SUMMARY OF RESULTS

As mentioned earlier, the primary emphasis for this investigation (NASA Contract NAG8-779) was given to ground-based research such as composition selection, glass preparation, construction of experimental apparatus, and determination of fluorescence concentration quenching. The results derived from the experiments conducted in a two year period for the work supported by this contract (NAG8-779) and described in detail in Section III are summarized below.

1. Two laser glass compositions in the silicate and phosphate systems, namely, $60.14SiO_2$-$2.53Al_2O_3$-$27.32Li_2O$-$9.86CaO$-$0.15CeO_2$, and $50P_2O_5$-$3Al_2O_3$-$27Li_2O$-$20CaO$, mol%, were developed for use in flight experiments. The processing parameters such as the melting temperature, heating rate, cooling rate, and processing time for these glasses are well within the capability of the flight facilities (furnaces) presently available.

2. The density for the silicate and phosphate glasses mentioned in 1 above was ~2.35 and ~2.9 g/ml, respectively, and increased with increasing Nd_2O_3 content in the glass.

3. The refractive index for these silicate and phosphate glasses was ~1.561 and ~1.531, respectively, and, like density, also increased with increasing Nd_2O_3.

4. Instruments required to measure the fluorescence spectra and fluorescence properties were designed and constructed.

5. The optical absorption and fluorescence spectra of Nd^{3+} ions in these glasses were measured in the wavelength range 400 to 900 and 800 to 1200 nm, respectively. The absorption

spectra for the silicate and phosphate glasses were very similar and independent of the Nd_2O_3 concentration, at least, up to the concentration used in the present investigation (maximum 2 mol% in the silicate and 4 mol% in the phosphate glass). The fluorescence spectra for these glasses were also independent of the Nd_2O_3 concentration but were slightly different for the two glasses. For example, the Nd^{3+} fluorescence for the $^4F_{3/2} \rightarrow {}^4I_{11/2}$ transition for the silicate and phosphate glasses appeared at $\sim$1062 and 1052 nm, respectively. The fluorescence linewidth for the phosphate glasses ($\sim$265 cm^{-1}) was much narrower compared to that for the silicate glasses ($\sim$340 cm^{-1}), but the linewidths for each glass family remained nearly unchanged with Nd_2O_3 concentration.

6. The measured lifetime, τ_f, for the Nd^{3+} fluorescence at 1060 nm decreased with increasing Nd_2O_3 for both the glasses, the rate of decrease for the silicate glasses being larger. This indicates that the effect of concentration quenching is larger in the silicate glasses compared to that in the phosphate glasses.

7. The limit of concentration quenching determined from the measurements of fluorescence intensity at 1060 nm was $\sim 2.85 \times 10^{20}$ and 9.00×10^{20} Nd^{3+} ions/ml for the phosphate and silicate glasses, respectively. These ion concentrations correspond to Nd_2O_3 content $\sim$0.49 and 2.30, mol%, for the silicate and phosphate glasses, respectively.

8. The radiative properties such as the transition probability (A), branching ratio (β), radiative decay time (τ_r), emission cross section (σ_p), and quantum efficiency (η_c) of Nd^{3+} in these glasses were calculated from absorption measurements using Judd-Ofelt (J-O) technique for the transitions $^4F_{3/2} \rightarrow {}^4I_{9/2}$, $^4I_{11/2}$, $^4I_{13/2}$, and $^4I_{15/2}$ which correspond to emissions at $\sim$880, 1060, 1350, and 1800 nm, respectively. Except the quantum efficiency, η_c, all these properties were, generally, independent of Nd_2O_3 concentration but depended strongly on the base glass composition. Like the measured fluorescence lifetime, τ_f, η_c decreased with increasing Nd_2O_3

concentration, demonstrating the effect of concentration quenching in the glasses. The calculated radiative properties of Nd^{3+} for the silicate glass containing 0.5 mol% Nd_2O_3 were in excellent agreement with those reported for a commercial glass of similar composition (Owens-Illinois, ED-2).

9. Ideally, the measured fluorescence lifetime, τ_f, should approach the radiative lifetime, τ_r, as the concentration, N, of the Nd^{3+} ions in the glass approaches zero. From the present measurements, the value of τ_f was determined for the silicate and phosphate glasses in the limit $N \rightarrow O$ as $\sim$400 and 280 μs, respectively, which are very close to the value of τ_r calculated for these glasses, namely, 394 $\pm$ 26 and 287 $\pm$ 7 μs, respectively.

10. A plot of $N \cdot \eta_c$ vs. N yielded a curve similar to those of I_f vs. N which is used to determine the limit for concentration quenching, N_L. N_L determined from the $N \cdot \eta_c$ vs. N plot was very close (within 3 to 5%) to that determined from the I_f vs. N plot. The use of $N \cdot \eta_c$ vs. N plot is recommended to determine the limit of concentration quenching, especially, for small glass samples such as those presently obtained from containerless experiments in space or on earth, since the measurements for $N \cdot \eta_c$ vs. N plot do not require any precise control for the preparation of samples as opposed to what is required for the measurements of I_f.

11. As determined by DTA and XRD, the crystallization behavior of the silicate glasses was independent of Nd_2O_3 concentration. Devitrification of these glasses leads to the crystallization of $Li_2O \cdot SiO_2$, $3CaO \cdot Al_2O_3 \cdot 3SiO_2$, and β-quartz solid solution. The crystallization of the phosphate glasses was much more complicated and was dependent upon the concentration of Nd_2O_3. These glasses were more resistant to crystallization than the silicate glasses and found to crystallize primarily by surface crystallization. Due to the complex nature of the XRD patterns, the crystallized phases for the phosphate glasses could not be identified.

12. The higher concentration limit for fluorescence self-quenching, larger emission cross section and lower tendency towards devitrification for the phosphate glass suggest that the phosphate glass is a superior host material than the silicate glass for Nd^{3+} solid state laser applications.

13. The scientific and technical informations obtained for these laser glasses in this research are considered significant. These data will be useful for planning flight experiments in space.

V. COMMENTS

The primary objective of this research was to study the feasibility of improving the fluorescence properties, particularly, the limit for concentration quenching for laser glasses prepared in the microgravity environment of space. The practical advantage of this research would be to prepare laser glasses (in microgravity) whose output power per unit volume should be several times higher than what is presently available for glasses prepared on earth. To accomplish the objectives of this research, glasses are needed to be prepared in space and the relevant properties of these space-melted glasses are to be measured and compared with those of the identical glasses prepared on earth.

During the two year period of the present research (Contract NAG8-779), attention was directed to ground-based investigation whose primary purpose was to determine the suitability and conditions for processing these laser glasses in space. This research was also aimed at developing techniques that would be suitable for handling and analyzing post-flight samples. This report describes that the scientific and technical information required for planning flight experiments for these glasses have been obtained, and the preparations for handling and

analyzing post-flight samples have also been taken. Laser glass compositions whose processing parameters are well within the capability of the flight instruments presently available, have been developed. Instruments required for measuring the fluorescence properties of interest have been constructed. The optical and fluorescence properties for the glasses which have been planned to process in space, have been measured and made available for comparative property analysis. Techniques to obtain reliable fluorescence data even for small samples (< 6 mm diameter) have been developed, should the samples obtained from flight experiments are restricted to small size. To accomplish the final objective of this work, i.e., to study the feasibility of improving the fluorescence efficiency and output power for laser glasses prepared in microgravity, a Flight Investigator Proposal has been submitted to the National Aeronautics and Space Administration (NASA) in response to the announcement NRA-91-OSSA-20 of 30 August 1991. If this request is granted, laser glasses containing different concentration of Nd_2O_3 will be prepared in space. The optical and fluorescence properties for the flight samples will be measured using the instruments and techniques developed in this ground-based research. A comparison of these properties for the flight samples with those determined in this investigation for the identical glasses prepared on earth will indicate the extent to which the fluorescence properties for the glasses prepared in space could be improved.

VI. ACKNOWLEDGEMENT

The author wishes to thank the National Aeronautics and Space Administration (NASA) for providing financial support for this research. Thanks are also due to Dr. Delbert E. Day for many helpful discussions and suggestions, and to Dr. X. J. Xu for technical assistance.

VII. REFERENCES

1. E. Snitzer, "Glass Lasers", Proc. Instn. Elect. Electron. Engrs., 54, 1249 (1966).
2. E. Snitzer and C. G. Young, "Glass Lasers", in Lasers, Ed. A. K. Levine, Vol. 2, Chapter 2, Marcel Dekker (1968).
3. K. Patek, "Glass Lasers", Ed. J. G. Edwards, CRC Press (1970).
4. E. Snitzer, Appl. Optics, 5, 121 (1966).
5. W. W. Etzel, H. W. Gandy, and R. J. Ginther, Appl. Optics, 1, 534 (1962).
6. E. Snitzer and R. Woodcock, Appl. Phys. Lett., 6, 45 (1965).
7. H. W. Gandy and R. J. Ginther, Proc. Inst. Radio Engrs., 50, 2113 (1962).
8. H. W. Gandy and R. J. Ginther, Appl. Phys. Lett., 1, 25 (1962).
9. M. J. Weber, J. Non-Cryst. Solids, 42, 189 (1980).
10. C. Hirayama, F. E. Camp, N. T. Melamed, and K. B. Steinbruegge, J. Non-Cryst. Solids, 6, 342 (1971).
11. G. E. Peterson and P. M. Bridenbaugh, J. Optical Soc. America, 54, 644 (1964).
12. L. G. Van Uitert and L. F. Johnson, J. Chem. Phys., 44, 3514 (1966).
13. G. T. Petrovskii, V. V. Ryumin, and I. V. Semeshkin, Steklo i Keramika (Glass and Ceramics), 1, 5 (1983) (English translation from Russian by Plenum Publishing Corporation).
14. C. Barta, L. Stourac, A. Triska, J. Kocka, and M. Zavetova, J. Non-Cryst. Solids, 35-36, 1239 (1980).
15. C. Barta, A. Triska, V. Ilyukhim, and G. Zhukov, Proc. 4th European Symp. on Mat. Sci. Under Microgravity Conditions, Madrid, Spain, 5-8 April (1983), p. 79 (ESA SP-191, 1983).

16. V. Braetsch and G. H. Frischat, Proc. 6th European Symp. on Mat. Sci. Under Microgravity Conditions, Borfeaux, France, 2-5 December (1986), p. 259 (ESA SP-256, 1987).

17. C. S. Ray and D. E. Day, Mat. Res. Soc. Symp. Proc., 87, 239 (1987).

18. W. F. Krupke, IEEE J. Quantum Electron., QE-10, 450 (1974).

19. R. R. Jacobs and M. J. Weber, IEEE J. Quantum Electron., QE-12, 102 (1976).

20. G. F. Neilson and M. C. Weinberg, J. Non-Cryst. Solids, 23, 43 (1977).

21. G. F. Neilson and M. C. Weinberg, J. Non-Cryst. Solids, 28, 209 (1978).

22. D. E. Day and C. S. Ray, NASA Technical Memorandum 4069, Vol. 2, October 1988, pp. 537-556.

23. G. J. Linford, R. A. Saroyan, J. B. Trenholm, and M. J. Weber, IEEE J. Quantum Electron., QE-15, 510 (1979).

24. C. Hirayama, F. E. Camp, N. T. Melamed, and K. B. Steinbruegge, J. Non-Cryst. Solids, 6, 342 (1971).

25. W. T. Carnall, P. R. Fields, and K. Rajnak, J. Chem. Phys., 49, 4424 (1968).

Table I. Fluorescence properties of the LG and LP glasses.

Nd_2O_3 Contents (mol%)	Measured Fluorescence Linewidth $\Delta\lambda_{eff}$ (cm^{-1})	Calculated Induced-emission Cross Section σ_p (10^{-20} cm^2)	Measured Fluorescence Lifetime in μsec $(\tau_f)_1$	$(\tau_f)_2$	Average, τ_f
Silicate glass					
0.25	346	2.5	360	361	360.5
0.50	339	2.3	299	300	299.5
1.00	337	2.2	113	191	113.0*
2.00	334	2.4	34	98	34.0*
Phosphate glass					
0.25	275	4.2	248	246	247.0
0.75	258	4.4	210	215	212.5
1.00	271	4.2	170	178	174.0
2.00	258	4.4	143	148	145.5
3.00	267	4.3	94	98	96.0
4.00	263	4.1	58	64	61.0

Base composition for LG (silicate) glass: $60.14SiO_2$-$27.32Li_2O$-$2.53Al_2O_3$-$9.86CaO$-$0.15CeO_2$, mol%

Base composition for LP (phosphate) glass: $50P_2O_5$-$27Li_2O$-$20CaO$-$3Al_2O_3$, mol%

*The first short decay time component, $(\tau_f)_1$, was used as τ_f, see text.

Table II. Intensity parameters for the LG and LP glasses containing different amount of Nd_2O_3, calculated using Judd-Ofelt (J-O) technique.

Nd_2O_3 Content (mol%)	Intensity Parameters (10^{-20} cm^2) Ω_2	Ω_4	Ω_6
Silicate glass			
0.25	2.75	4.75	4.96
0.50	3.38 (3.30)*	3.82 (4.68)*	4.52 (5.18)*
1.00	3.13	4.02	4.32
2.00	2.83	4.39	4.40
Phosphate glass			
0.25	4.00	6.71	7.00
1.00	4.00	6.52	6.73
2.00	4.02	6.21	6.81
3.00	4.20	6.40	6.50
4.00	3.91	6.43	6.97

For composition of LG and LP glasses, see text and Table I.
*Values in parentheses are for the commercial ED-2 glass (ref. 18) whose composition is close to the present composition shown.

Table III. Radiative emission properties for transitions $^4F_{3/2} \rightarrow {}^4I_{9/2,\ 11/2,\ 13/2,\ 15/2}$, for Nd^{3+} in the LG and LP glasses, calculated using Judd-Ofelt (J-O) technique.

Nd_2O_3 Contents (mol%)	Spontaneous Emission Probability (sec^{-1})				Branching Ratio				Radiative Lifetime τ_r (μsec)	Average, τ_r (μsec)
	$A_{0.88}$	$A_{1.06}$	$A_{1.35}$	$A_{1.88}$	$\beta_{0.88}$	$\beta_{1.06}$	$\beta_{1.35}$	$\beta_{1.88}$		
Silicate Glass										
0.25	1042	1411	266	10	0.38	0.51	0.10	0.004	367	
0.50	864 (1030)	1256 (1380)	245 (272)	9 (12)	0.36 (0.38)	0.53 (0.51)	0.10 (0.10)	0.004 (0.004)	420	396 ± 26 (372)
1.00	900	1241	236	9	0.38	0.52	0.10	0.004	420	
2.00	991	1315	246	9	0.39	0.51	0.10	0.004	390	
Phosphate Glass										
0.25	1368	1854	350	13	0.38	0.52	0.10	0.004	279	
0.75	1311	1817	347	13	0.38	0.52	0.10	0.004	287	
1.00	1347	1814	342	13	0.38	0.52	0.10	0.004	285	287 ± 7
2.00	1306	1819	348	13	0.37	0.53	0.10	0.004	287	
3.00	1254	1793	347	13	0.37	0.53	0.10	0.004	293	
4.00	1261	1824	355	13	0.37	0.53	0.10	0.004	290	

For LG and LP glass compositions, see text (Section IIIA) and Table I. Values in parentheses are for the commercial ED-2 glass (ref. 18) whose composition is close to the present composition shown.

Table IV. Limit of Nd^{3+} ion concentration for fluorescence self-quenching, N_L, in the LG and LP glasses.

Glass	N_L From I_f vs. N plot (Fig. 9a) 10^{20} ions/cm^3	N_L From I_f vs. N plot (Fig. 9a) Mol% Nd_2O_3	N_L From $N \cdot \eta_c$ vs. N plot (Fig. 9b) 10^{20} ions/cm^3	N_L From $N \cdot \eta_c$ vs. N plot (Fig. 9b) Mol% Nd_2O_3
Silicate	2.65	0.49	2.85	0.50
Phosphate	8.50	2.30	9.00	2.50

For LG and LP glass compositions, see text (Section IIIA) and Table I.